Vibrissal growth parameters of southern elephant seals *Mirounga leonina*: obtaining fine-scale, time-based stable isotope data

Nico Lübcker[1*], Richard Condit[2], Roxanne S. Beltran[3,4], P.J. Nico de Bruyn[1], Marthán N. Bester[1]

[1] Mammal Research Institute, Department of Zoology and Entomology, University of Pretoria, Private Bag X20, Hatfield 0028, Pretoria, South Africa.

[2] Smithsonian Tropical Research Institute, Balboa, Panama City, 0843-03092, Panama.

[3] Department of Biological Sciences, University of Alaska, Anchorage, AK 99508, USA.

[4] Department of Biological Sciences, University of Alaska, Fairbanks, AK 99775, USA.

* Author for correspondence: nlubcker@zoology.up.ac.za

Running head: Vibrissal growth parameters of southern elephant seals

ABSTRACT

Stable isotopes provide a powerful, indirect approach to assess the trophic ecology of individuals on a spatial and temporally integrated basis (especially when combined with telemetry). However, using stable isotopes requires accurate, species-specific quantification of the period of biomolecule deposition in the sampled tissue. Sequentially sampled vibrissae (whiskers) provide a chronology of biogeochemical data, although knowledge of the vibrissal growth is required for temporal interpretations. We sampled vibrissae from southern elephant seals (*Mirounga leonina,* hereafter SES) at Marion Island, southern Indian Ocean to address the following aims: define the prevalence and timing of their vibrissal replacement; determine the vibrissal regrowth rate and temporal resolution of isotopic data captured along the length

of sequentially sampled vibrissae; and explore assumptions regarding their vibrissal growth. Contrary to the previously described asynchronous vibrissal shedding pattern of SES, 71.1 % of individuals displayed vibrissal shedding during the annual pelage moult. Furthermore, vibrissa growth ceased once the asymptotic length was reached, and the vibrissae were retained before being replaced. Vibrissae with known growth histories were re-sampled at multiple, known intervals to control for unknown growth starting dates. Vibrissae followed a von Bertalanffy growth function [$G_t = 77.1\,(0.00744)(e^{-0.00744t})$], as the growth rate decreased near the asymptotic length. The resolution of the isotopic data obtainable per 2 mm section ranged from 3.5 days at the vibrissal tip to > 40 days at the base. Using these defined growth rates and shedding patterns, researchers can prudently apply timestamps to stable isotope values along vibrissae.

Keywords: Biomonitoring; marine mammals; moult; pinnipeds; shedding; whiskers

INTRODUCTION

The combination of stable isotopes (SIs) and satellite-linked telemetry enables fine-scale, spatio-temporal dietary analyses, and biogeochemical habitat characterisations (Hobson et al. 2004; Jaeger et al. 2013; McMahon et al. 2013; Young et al. 2015; reviewed in Hussey et al. 2015). However, such a combined approach requires higher resolution SI data (Beltran et al. 2015; also see Banks et al. 2014). The SI signature captured along the length of keratinous tissue, such as feathers (Grecian et al. 2015), nails, hair or vibrissae, provides a time-series of the species' dietary history, if analysed chronologically (Hückstädt et al. 2012; Robertson et al. 2012; Walters et al. 2014; Beltran et al. 2015). Numerous studies focussed on ascertaining the exact, species- and tissue-specific growth rates of slow-growing, biologically inert

keratinous tissue of various species in different habitats (e.g., Greaves et al. 2004; Rohwer et al. 2009; Beltran et al. 2015).

The vibrissae (whiskers) of pinnipeds (Ling 1966) are particularly useful for dietary studies when using SI analysis (e.g., Hirons et al. 2001; Greaves et al. 2004; Zhao & Schell 2004; Hall-Aspland et al. 2005; Lewis et al. 2006; Cherel et al. 2009; Hindell et al. 2012; Walters et al. 2014; Rea et al. 2015). Vibrissae can be sampled relatively non-invasively and archive ecological information over longer temporal scales at a finer resolution than other tissues, such as blood (Tieszen et al. 1983). Whole blood, for example, has an isotopic turnover rate of *ca*. 1 month (Tieszen et al. 1983), and consequently represents a single, integrated measurement of all the prey consumed during the month preceding sampling (e.g., Cherel et al. 2008; Boecklen et al. 2011). In contrast, the half-life of an isotopic tracer injected in captive harbour seals *Phoca vitulina,* was 47.1 days (Zhao & Schell 2004), although isotopic changes were visible after four days which implies that the marker incorporates rapidly into the protein synthesis of the growing vibrissae (Hirons et al. 2001). As a result, vibrissae are increasingly utilised to study the diet of pinnipeds (Greaves et al. 2004; Hückstädt et al. 2011, 2012; Newland et al. 2011; Hindell et al. 2012; Walters et al. 2014). Nevertheless, the vibrissal growth rates of several phocid species remain to be determined, despite the recent interest in the utilisation of vibrissae to increase the temporal resolution of the dietary data (e.g., Hirons et al. 2001; Greaves et al. 2004; Zhao & Schell 2004; Hall-Aspland et al. 2005; Beltran et al. 2015).

The growth rate and retention period of vibrissae vary between otariid and phocid species (Greaves et al. 2004). The vibrissae of otariids, such as Antarctic fur seals *Arctocephalus gazella* (Walters 2014), and Steller sea lions *Eumetopias jubatus* (Hirons et al. 2001), grow linearly and are retained for multiple years (Hirons et al. 2001; Cherel et al. 2009;

Kernaléguen et al. 2012). In contrast, the vibrissae of phocids, such as grey seals *Halichoerus grypus,* and *P. vitulina*, grow asymptotically and are characterised by an asynchronous growth and replacement pattern (Greaves et al. 2004; Hall-Aspland et al. 2005; Beltran et al. 2015). Furthermore, it is suggested that vibrissae of phocids have short retention times; for example, *P. vitulina* and spotted seals, *Phoca largha*, shed their vibrissae on an annual basis (Zhao & Schell 2004; McHuron et al. 2016).

Southern elephant seals (*Mirounga leonina*, hereafter SES) are the most abundant phocid in the sub-Antarctic region, and although their vibrissae have been used in dietary studies (Cherel et al. 2008; Hückstädt et al. 2011; Newland et al. 2011; Walters et al. 2014), the growth rate and shedding pattern (Ling 1966) of their vibrissae remains poorly understood. Whether the vibrissae of SES grow continuously before being replaced (Ling 1966), or enter an inactive phase after reaching the maximum length (Newland et al. 2011), remains debated. Also not yet enumerated, although generally accepted, is that individual vibrissae display asynchronous growth and replacement patterns (Ling 1966; Walters et al. 2014) (see Supplementary figures, plate 1S). The ability to obtain fine-scale, temporal integrated biogeochemical data was demonstrated in a similar study conducted on a single, captive adult female northern elephant seal, *Mirounga angustirostris* (Beltran et al. 2015). However, ascertaining the starting date of the vibrissal growth remains a prerequisite to assign dates to dietary data (Greaves et al. 2004). Resampling of vibrissal regrowths after initial sampling can help to account for unknown growth histories (e.g., Walters 2014).

The aim of this was to: 1) determine the shedding phenology of SES vibrissae; 2) describe the vibrissal growth parameters and temporal range of data capture along the vibrissal regrowths of known-aged SES; 3) quantifying the degree of inter-vibrissae isotopic variation to assess the degree of synchronous vibrissal growth; and 4) determine if the isotopic composition of

the proximal sections of vibrissae are influenced by the presence of molecules other than pure keratin in the metabolically active inner vibrissal root sheath (Ling 1966; Hückstädt et al. 2011). We hope to quantify the temporal resolution of isotopic data captured along the length of SES vibrissae and provide guidelines for future sampling. We additionally explore previous assumptions that have been made in past studies using samples collected from various age-class SES.

METHODS

Study site and data collection

Samples were collected at Marion Island in the southern Indian Ocean (46.88° S, 37.87° E) during the 2012/2013 and 2013/2014 breeding season and annual pelage moult, as part of the long-term (1983 – ongoing) SES mark-recapture programme (Bester & Wilkinson 1994; de Bruyn et al. 2008; Bester et al. 2011; Pistorius et al. 2011). During the moult haulout (mid-August to mid-April), censused individuals were assigned to one of the following moult categories: unmoulted, < 1/3rd moulted, 1/3-2/3rd moulted, > 2/3rd moulted, and fully moulted. For the purpose of this manuscript, 'moulting' describes the action of their annual pelage moult, while 'shedding' is used to describe the vibrissal loss-replacement of SES studied herein.

Timing and prevalence of vibrissal shedding

Body and snout photographs of marked individuals were routinely obtained as part of a concurrent photogrammetry study during the 2012/2013 and 2013/2014 moult periods (Postma et al. 2013). At each photograph sampling occasion, mystacial beds of each individual were assigned to one of the following vibrissal shedding categories: a) not shed, when most of the anterior vibrissae were present and > 4 of posterior vibrissae were present

on either side; b) partially shed, when the anterior vibrissae were all shed but > 4 of posterior vibrissae were present on either side; or c) completely shed, when ≤ 4 of the posterior vibrissae were present on either side of the face (Figure 1, Supplementary plates 1S, 2S, and 3S). We also noted the number of cases where new vibrissal regrowths were visible (Supplementary figures, plate 4S). We excluded males >3 yo from analyses because adult males are rarely observed with a full set of vibrissae due to proboscis development and increased fighting (Ling 1966).

To avoid sampling biases due to the timing of the vibrissal shedding when calculating the prevalence of the observed shedding, animals were only included in the analysis if they were observed in at least two different moult stages during one moulting season. Furthermore, the individual should have been observed at least once at the onset of the annual pelage moult (i.e., unmoulted or < $1/3^{rd}$ moulted), and once after (i.e., fully moulted). The vibrissal shedding status of an individual SES was then based on the progression from one state (not shed, partially shed, or completely shed) to the next, in successive observations. For instance, if the individual was initially observed with a full vibrissal complement, then with a partially shed vibrissal aggregate, and recaptured on a third occasion with no vibrissae, we counted the individual's vibrissae as 'completely shed' during the moult. 'No shedding' occurred when the full vibrissal aggregate was observed during successive recaptures in one season. A non-parametric Kruskal-Wallis χ^2 test was utilized to identify any significant differences between the duration of the moult haulout and the number of observations between individuals that shed their vibrissae (completely or partially) and those that did not. The duration of the moult haulout for each individual was based on the number of days that elapsed between first and last recapture during the routinely conducted censuses, following Kirkman et al. (2003).

Growth rate of re-sampled vibrissae

To overcome the limitations of sampling vibrissae for which the onset of biomolecule deposition is unknown, we collected (by cutting as close to the skin as possible) the longest mystacial vibrissa from the right-hand side of recently weaned SES pups (*ca.* 22 – 24 days old). Either vibrissa C1, C2 or D1 was sampled (Figure 1, Sadou et al. 2014). The collection date, vibrissa bed location and length of the initial 'cut-off' vibrissa were recorded for each tagged individual. A ruler was used to measure the length of the vibrissal regrowths of recaptured post-weaning SES (n = 101) on different occasions during the 60-day post-weaning period (Wilkinson & Bester 1990). After spending their first year foraging at sea (Kirkman et al. 2003), juveniles with visible regrowths were recaptured (n = 43) and the regrown vibrissae were again sampled by cutting as close to the skin as possible. These vibrissae were easily identified by their blunt distal ends (Supplementary figures, plate 5S).

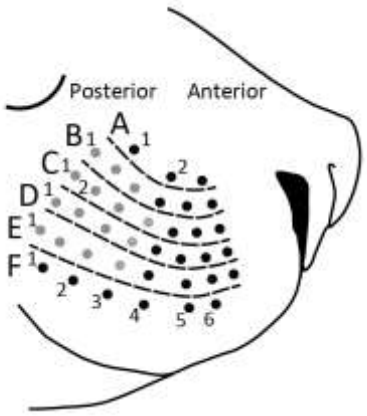

Figure 1: Southern elephant seal (SES) mystacial vibrissal arrangement. The posterior vibrissae are more prominent (grey circles) then the anterior vibrissae (black), and can reach up to 160 mm in length. The diagram was modified from Sadou et al. (2014) following the description of the SES mystacial vibrissal arrangement in Ling (1966). Vibrissa C1, C2, or D1, was sampled from juvenile SES in order to determine their vibrissal regrowth rate.

Our starting assumption was that vibrissal regrowth in the post-weaned SES was nonlinear, based especially on detailed vibrissal growth measurements of the closely related *M. angustirostris* (Beltran et al. 2015). The vibrissal growth rate of *M. angustirostris* always decelerated until reaching the asymptotic length after about one year (Beltran et al. 2015). The decay in the growth rate was subsequently demonstrated using the widely applicable von Bertalanffy growth function (e.g., Hall-Aspland et al. 2005; Armstrong & Brooks 2013; Beltran et al. 2015). Although the growth rate model of Beltran et al. (2015) was based on an adult female, our preliminary results clearly demonstrated a similar decelerating growth pattern. We thus held the assumption that the von Bertalanffy growth model was our best option. Given decelerating growth, we needed at least three measurements to fit the model, and we included 19 juvenile SES for which we had ≥ 3 measurements that spanned a minimum of 200 days after weaning.

We fitted the von Bertalanffy function (Equation 1) to the length of all 19 animals' vibrissae jointly, treating the individual as a random effect.

The model was thus specified by:

$$Length \sim \text{VonB}(time + time|seal) + \epsilon \quad (1)$$

indicating that length was modelled as a function of time using the von Bertalanffy function, with the seal as a random effect, and a normally-distributed error ϵ.

The general von Bertalanffy function is:

$$S_\rho(T) = A\left(1 - e^{-K(T-T_0)}\right) \quad (2)$$

where S_ρ represents the predicted length at time T given three parameters: A, asymptotic length; $K > 0$, the curvature parameter; and T_0, the time at which growth begins (so $S_\rho = 0$). Since we cut the vibrissae to the skin, we set $T_0 = 0$ and estimate only K and A. The model parameters include a fixed effect $\theta_F = (A_F, K_F)$, the best estimate for all 19 animals together (average), plus a separate set of parameters $\theta_i = (A_i, K_i)$, for each animal i. There must be a hyperdistribution for θ_i, describing the variance between animals, which we assumed to be bivariate Gaussian. To allow the Gaussian assumption, a log-transformation for K was necessary because it is always a very small positive number, and a normal distribution would allow negative values. Thus, the fitted model parameters were log K and A, but we always back-transformed and display only K, not log K. The asymptote A was also constrained to be > 0, however it never approached 0, so the Gaussian distribution is adequate. One additional parameter needed for the model was ϵ, or the residual standard deviation of the error around the model, again assumed to be Gaussian.

Estimating parameters required one likelihood function for the observations, describing the probability P_{ij} of observing seal i's vibrissa on day j as size S_{ij}, given predicted size S_ρ based on the model and parameters θ_i for seal i, plus the residual Gaussian error,

$$P_{ij} = \text{dnorm}(S_{ij}, \text{mean } = S_p(\theta_i), sd = \epsilon) \quad (3)$$

where dnorm is the standard normal deviate given the mean and standard deviation (sd). Equation (3) must be repeated for every measurement of every seal i, and the log-likelihood of all observations is $\sum_{ij} logP_{ij}$

There are two additional likelihood functions for the fixed effects, θ_F,

$$P_{Ai} = \text{dnorm}\left(A_i, \text{mean} = A_f, \text{sd} = \sigma_A\right)$$

$$P_{\log K} = \text{dnorm}(\log K, \text{mean} = \widehat{log\ K}, \text{sd} = \sigma_{log\ K}) \quad (4)$$

where A_f is the hyper-mean and σ_A are the hyper-standard-deviation of 19 regrowths' asymptote lengths, and likewise for the hyper-mean and hyper-SD of $\log K$, $\widehat{log\ K}$, and $\sigma_{log\ K}$.. The log of the two probabilities in Equation (4) must be summed over each animal *i*. The total log-likelihood for the entire set of observations, given an entire set of parameters θ_i and θ_F, is

$$\Pi = \sum_i logP_{Ai} + \sum_i logP_{log\ K_i} + \sum_{ij} logP_{ij} \quad (5)$$

Parameters were estimated in a Bayesian framework, using Metropolis updates based on the full likelihood formulation (Equation 5). The entire set of parameters was updated 25000 times, and the first 5000 discarded as burn-in. The remaining 20000 values describe posterior distributions for every parameter. Credible intervals (95 %) for each were defined as the central 95 percentiles of these distributions. The individual parameters A_i and K_i were used to describe growth trajectories for all 19 seals' vibrissae. In addition, given the von Bertalanffy formulation, with $T_0 = 0$, vibrissa growth rate at time *T* can be calculated as:

$$_T = AKe^{(-KT)} \quad (6)$$

Posterior distributions of A_i and K_i were converted into posterior distribution of growth rates at day 0 and day 40 for each seal, with associated 95 % credible intervals.

The resolution (number of days) represented by a 2 mm vibrissal segment was determined using Equation (7),

$$T = \left[\frac{-1}{K}\ln\left(1 - \frac{S_T}{A}\right)\right] + T_0 \quad (7)$$

where S_T represents the length of the regrowth at time T (Beltran et al. 2015). Vibrissae are often subsampled into 2 mm segments for isotopic analyses (e.g., Newland et al. 2011; Walters et al. 2014), and we therefore reported the average number of days represented by a 2 mm vibrissal segment to emphasize the temporal resolution of the biogeochemistry data obtainable from sequentially sampled vibrissae.

We additionally used the length of the resampled regrowth to calculate the linear growth of the vibrissae for the 19 juvenile SES, for comparative purposes with Walters (2014).

Testing assumptions regarding vibrissal growth using stable isotopes

We assessed the δ^{13}C and δ^{15}N isotope profile captured along the length of previously unsampled vibrissa from one 1.7 year old SES (hereafter, Seal 1) and a regrowth of a 1.1 year old SES (hereafter, Seal 2) to confirm if a) the vibrissal growth as asynchronously; b) vibrissae are retained for some period once their maximum length is reached; and c) the maternally derived SI signature are still observable in the vibrissae juvenile SES.

To ensure that the SI signature is represented similarly across different vibrissae grown at the same time, we compared the SI profile of two vibrissae collected simultaneously from a third individual (hereafter, Seal 3, 0.8 yo) and eight vibrissae collected from a deceased adult female SES (hereafter, Seal 4) (see Lewis et al. (2006) and Newland et al. (2011)). We controlled for different vibrissa lengths and growth rates in Seal 4 (Greaves et al. 2004;

Beltran et al. 2015) by applying the growth rate of adult *M. angustirostris* from Beltran et al. (2015), using the maximum length of each of the sampled vibrissae as the asymptotic length in the equation.

Finally, to determine whether the vibrissae base is isotopically enriched due to the presence of molecules other than pure keratin, such as non-keratinized cortical cells (e.g., Hall-Aspland et al. 2005; Hückstädt et al. 2011), we compared the isotopic signature of the base (10 mm) of the eight vibrissae of Seal 4 to the adjacent 10 mm and to the most proximal *ca*. 10 mm using a Kruskal-Wallis χ^2 test, followed by a post-hoc Wilcoxon rank sum test.

To prepare and analyse samples for stable isotopes, each vibrissa was cleaned using a chloroform:ethanol rinse as described by Lewis et al. (2006). All samples were then oven-dried for 24 h at 70 $^{\circ}$C (Lowther et al. 2013), sequentially sub-sampled into 2 mm sections ranging from the proximal portion (base) to the distal portion (tip) following Hindell et al. (2012) and Walters et al. (2014). The 2 mm section was again sub-sampled, and 0.5 – 0.6 mg weighed into tin capsules (pre-cleaned in Toluene) for SI analysis. The remaining portion was weighed as duplicate, if a 0.5 – 0.6 mg sample was still available. Weighed sample aliquots were combusted in an elemental analyser (Flash EA, 1112 Series, Thermo™, Thermo Fisher Scientific, Bremen, Germany), and the δ^{13}C and δ^{15}N isotopes were determined using a continuous-flow isotope ratio mass spectrometer (Delta V Plus, Thermo Finnigan, Bremen, Germany) at the Stable Isotope Laboratory of the Mammal Research Institute, University of Pretoria, South Africa. Results are presented using standard delta notation in parts per thousand (‰) relative to an international standard: Vienna Pee Dee Belemnite (VPDB) for δ^{13}C and atmospheric N_2 (Air) for δ^{15}N (Coplen 1994).

Duplicate aliquots of samples were interspersed with an in-house standard (Merck gel) and blank after every 10 samples to ensure reproducibility. Reproducibility of $\delta^{13}C$ as well as $\delta^{15}N$ values based on the standards was < 0.20 ‰, while the reproducibility of duplicate aliquots was ± 0.20 ‰ for $\delta^{15}N$ and ± 0.16 ‰ for $\delta^{13}C$ (n = 81 duplicates). The atomic C:N ratios are reported throughout the manuscript.

All statistical tests were performed in the R environment (R Core Team 2013). We tested normality using a Shapiro-Wilks normality test, while the F-test was used to compare the variances between variables, before applying an appropriate parametric (Analysis of Variance (ANOVA)) or non-parametric test (Kruskal-Wallis χ^2). Values are presented as mean ± one standard deviation (SD) where applicable, and significance was assumed at $p < 0.05$.

RESULTS

Timing and prevalence of vibrissal shedding

From the total of 1289 facial photographs, 32.3 % and 67.7 % were conducted on males and females, respectively. Poor photo resolution, unknown moult stage, or obstruction of the vibrissae resulted in the exclusion of 162 observations. During the 30.1 ± 9.7 day moulting period, 62.3 % of the complete vibrissal shedding observations occurred during the post-moult stage (Figure 2). The probability of observing vibrissal shedding was strongly related to the pelage shedding stage (Figure 2), suggesting that the timing of the vibrissal shedding should be accounted for when calculating the prevalence of the vibrissal shedding.

The prevalence of the vibrissal shedding was based on 201 individuals (549 observations), consisting of 1 – 3 yo juvenile males (23.9 % of individuals); juvenile females (23.4 %); as well as adult females > 3 yo (52.7 %). Of the 201 individuals, 71.1 % displayed signs of

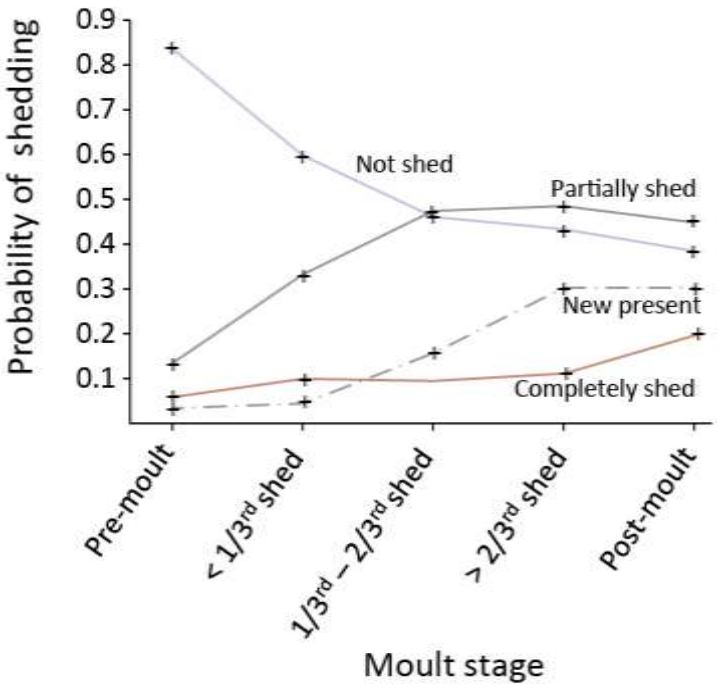

Figure 2: Prevalence of southern elephant seal mystacial vibrissal shedding during each pelage moult stage. The probability of observing vibrissal shedding depended on pelage moult stage, and complete vibrissal shedding (red) occurred most frequently at the end of the pelage moult.

vibrissal shedding during the annual moult (Supplementary figure 1S). The vibrissae were completely shed in 22.5 % of the individuals and partially shed in 48.5 %. Only 28.9 % of the individuals retained their vibrissae during the annual pelage moult. New vibrissal growths were observed in 56.4 % of individuals that shed their vibrissae. The prevalence of the vibrissal shedding was highest in age 2 individuals, with 59.2 % completely shedding their vibrissae (Supplementary figure 1S). The sighting probability and moult duration did not differ significantly (Kruskal-Wallis $\chi^2 = 1.38$, $df = 4$, $p = 0.85$; Kruskal-Wallis $\chi^2 = 32.93$, $df = 39$, $p = 0.74$, respectively) between individuals that completely, or partially shed, their vibrissae and individuals that did not. Individuals that shed their vibrissae were observed 2.9 ± 0.8 times within a given moult season; similar to the 2.6 ± 0.7 times of those that did not shed their vibrissae. The duration of the moult between individuals that shed their vibrissae (30.3 ± 9.9 days) was also similar to individuals that did not (29.0 ± 7.9 days). One individual

(hereafter, Seal 5) that completely shed all its vibrissae during the moult was recaptured 138 days later with a full vibrissal complement (Supplementary figures, plate 6S).

Growth rate of re-sampled vibrissae

The vibrissal regrowth rate of the known-aged SES (n = 19) represents a von Bertalanffy growth function (Figure 3); the vibrissal regrowth rate decreases exponentially [$G_t = 77.1\,(0.00744)(e^{-0.00744t})$], following from Equation 6. Results were reported as the mean, followed by the 95 % credible intervals (lower 95 percentile; upper 95 percentile in brackets), where applicable.The resampled regrowths were shorter (66.3 ± 12.2 mm) than the vibrissae originally cut off (75.7 ± 9.7 mm), while also shorter than the predicted *A* of the regrowths [77.1 (65.4; 89.9) mm], therefore suggesting that the vibrissal regrowths were still actively growing when sampled. The predicted *K* of the resampled regrowths was 0.00744 (0.0058; 0.0095).

The maximum growth rate [0.57 (0.47; 0.67) mm. day^{-1}] occurs directly after sampling the initial vibrissae (T_0 = 0), and decreased to 0.42 (0.37; 0.48) mm. day^{-1} after growing *ca.* 20 mm in 40 days (Table 1). The mean number of days represented by a 2 mm vibrissal segment when sampled was therefore 3.5 days (ranging from 2.4 to 5.5 days based on 95 % percent credibility intervals), and increased to 4.0 days (ranging from 3.5 to 6.3 days) after 40 days. The daily resolution decreases further towards the base of the vibrissae, averaging 10.3 days (ranging from 5.4 to 24.0 days) after growing *ca*. 52 mm, 150 days after the initial sampling. When regrowth approaches *A*, the resolution of the dietary data obtainable near the base of the regrowth is reduced to the average isotopic signature of all the prey consumed over > 40

Table 1: Estimates of the asymptotic length (A) and the growth curvature constant (K) of the individual southern elephant seal vibrissal regrowths (n = 19). The maximum measured length of the regrowth (L_m), length of the initial vibrissa cut-off after weaning (L_c), and the growth rate at time t = 0 days and after 40 days are also presented. The reported values represent the mean and 95 % credibility intervals (in brackets) of the parameters. The estimated growth parameters for one individual (YO092) were out of range of the maximum vibrissal length measured in SES.

Seal ID	K (day^{-1})	A (mm)	Growth rate at t = 0 days	Growth day at t = 40 days	Max L_m (mm)	L_c (mm)
YO009	0.00736 (0.0068,0.0080)	80.1 (78.4,81.9)	0.590 (0.55,0.63)	0.440 (0.42,0.46)	76	82
YO010	0.00899 (0.0084,0.0096)	84.3 (82.8,85.7)	0.758 (0.72,0.80)	0.529 (0.51,0.55)	82	94
YO012	0.00696 (0.0064,0.0075)	81.7 (79.8,83.7)	0.568 (0.53,0.61)	0.430 (0.41,0.45)	77	64
YO015	0.01260 (0.0114,0.0138)	47.5 (46.2,48.8)	0.599 (0.55,0.65)	0.361 (0.34,0.38)	47	71
YO024	0.00767 (0.0070,0.0084)	82.6 (80.8,84.4)	0.633 (0.58,0.69)	0.466 (0.44,0.49)	79	81
YO035	0.01269 (0.0115,0.0140)	50.4 (49.1,51.6)	0.643 (0.59,0.70)	0.385 (0.37,0.40)	50	54
YO039	0.00420 (0.0034,0.0049)	96.3 (90.1,104.9)	0.404 (0.36,0.45)	0.341 (0.31,0.37)	78	80
YO053	0.01070 (0.0094,0.0120)	47.7 (46.5,49.1)	0.513 (0.46,0.57)	0.332 (0.31,0.35)	47	68
YO059	0.00885 (0.0082,0.0095)	59.9 (58.5,61.4)	0.531 (0.50,0.57)	0.372 (0.36,0.39)	58	66
YO064	0.00975 (0.0092,0.0103)	71.5 (70.2,72.9)	0.698 (0.66,0.73)	0.472 (0.46,0.48)	70	77
YO067	0.00668 (0.0061,0.0073)	67.9 (66.0,69.9)	0.453 (0.43,0.48)	0.347 (0.33,0.36)	63	80
YO081	0.00739 (0.0067,0.0080)	93.8 (90.6,98.1)	0.694 (0.65,0.73)	0.515 (0.50,0.53)	79	72
YO089	0.00482 (0.0035,0.0066)	68.1 (61.6,77.5)	0.330 (0.27,0.40)	0.271 (0.23,0.31)	57	61
YO090	0.00845 (0.0071,0.0098)	80.1 (77.1,84.0)	0.678 (0.60,0.76)	0.482 (0.45,0.51)	73	77
YO092	0.00332 (0.0027,0.0043)	154.3 (131.3,177.7)	0.511 (0.48,0.56)	0.446 (0.43,0.47)	85	82
YO097	0.00236 (0.0015,0.0047)	107.7 (74.1,145.6)	0.252 (0.21,0.35)	0.226 (0.20,0.29)	62	86
YO264	0.00860 (0.0068,0.0102)	68.4 (64.6,74.3)	0.593 (0.51,0.66)	0.416 (0.39,0.44)	59	83
YO392	0.00774 (0.0064,0.0093)	60.9 (58.5,63.9)	0.472 (0.40,0.54)	0.345 (0.32,0.38)	57	80.5
YO404	0.01557 (0.0146,0.0166)	60.2 (59.0,61.4)	0.938 (0.88,0.99)	0.502 (0.49,0.51)	60	79

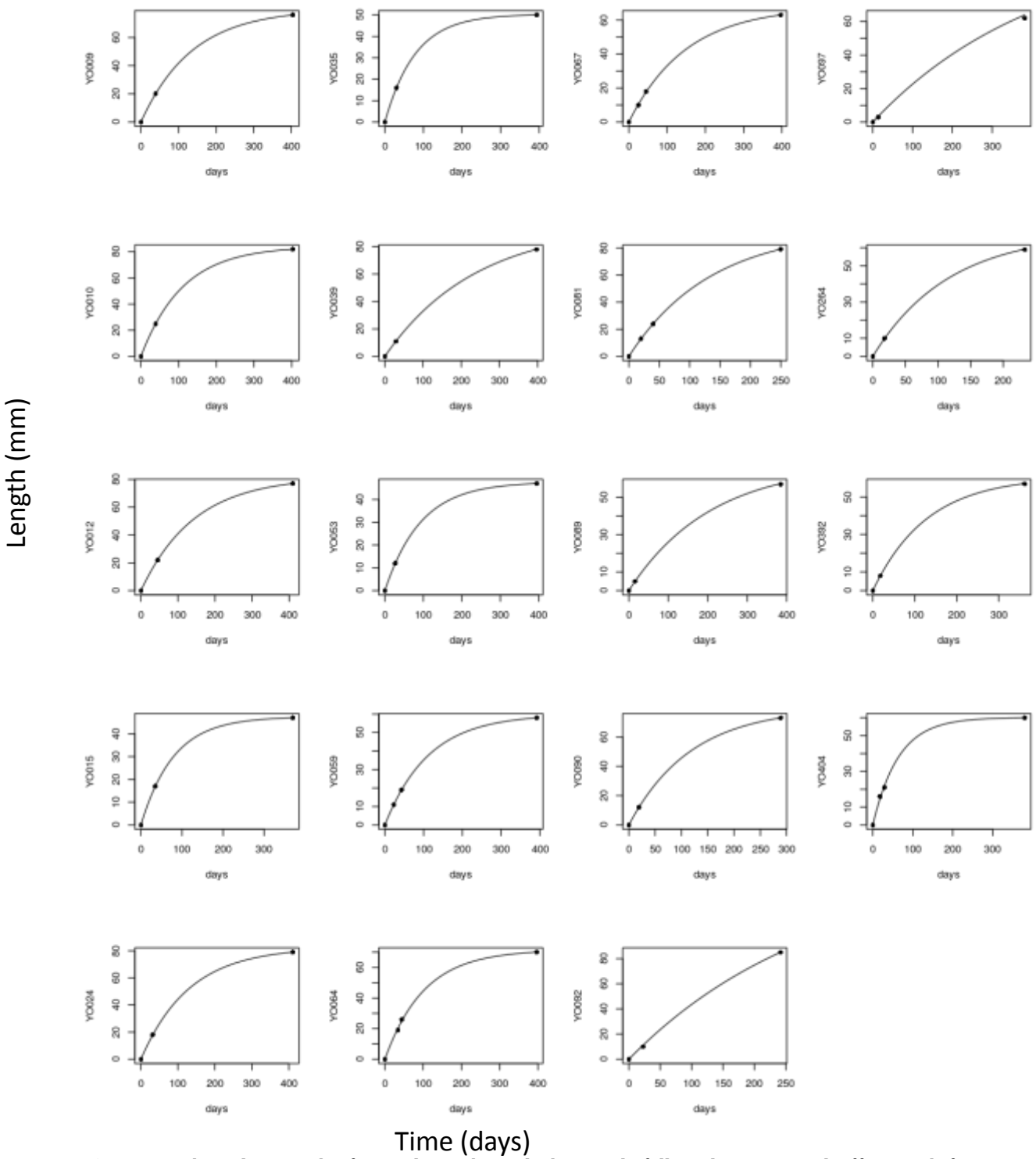

Figure 3: Vibrissal regrowth of juvenile southern elephant seals followed a von Bertalanffy growth function. The growth rate decreased as the asymptotic length was approached.

day period. Irrespectively, the estimated growth rate from a simple linear regression was 0.19 ± 0.06 mm. day^{-1}.

Testing assumptions regarding vibrissal growth using stable isotopes

Two vibrissae, each sub-sampled into 51 (Seal 1) and 35 segments (Seal 2), were used to assess the retention of the vibrissae in juvenile SES. The maternal signature was still present in the full vibrissa of Seal 1 at 1.7 yo (n = 51 samples), as well as in the regrowth sampled from the 1.1 yo Seal 2 (n = 35 samples) before the second moult (Figure 4), confirming that the vibrissae grew asynchronously and that they are retained for some period once their maximum length is reached. The maternal signature, and subsequent δ^{15}N depletion, represented 83 % of the total length of the vibrissa collected from Seal 2. Independent foraging was represented by 17 % of the vibrissal regrowth (Seal 2), while only represented by the last segment of Seal 1 (Figure 4).

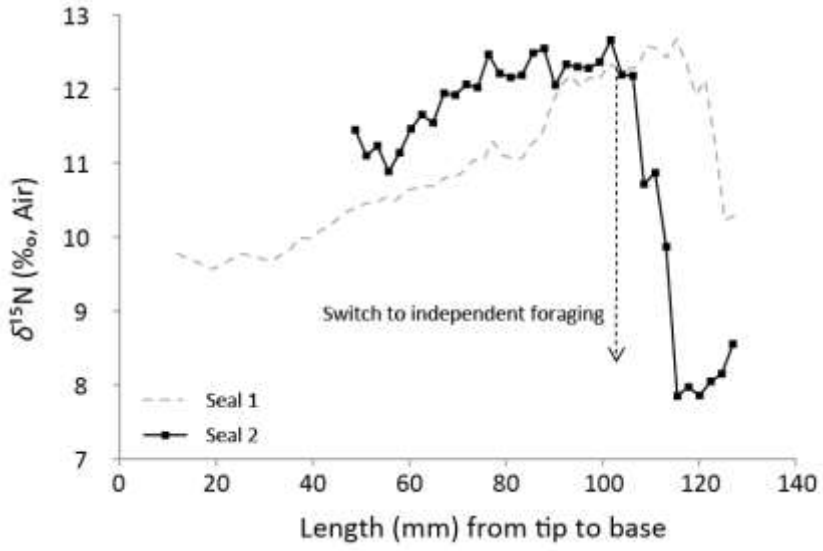

Figure 4: Pre-foraging trip isotopic signature and subsequent *ca.* 3.0 ‰ δ^{15}N decrease from nursing to independent foraging (Walters et al. 2014) was still observable in a 1.7 yo and 1.1 yo southern elephant seal (Seal 1 & 2, respectively). No evidence of a secondary growth spurt, or continuous growth to offset abrasion occurred.

The reproducibility of the δ^{15}N (10.6 ± 1.2 ‰) and δ^{13}C (-20.1 ± 0.2 ‰) profile along of the regrowth of Seal 3 was nearly identical to the δ^{15}N (10.7 ± 1.4‰) and δ^{13}C (-19.9 ± 0.3 ‰) of the duplicate regrowth (Figure 5).

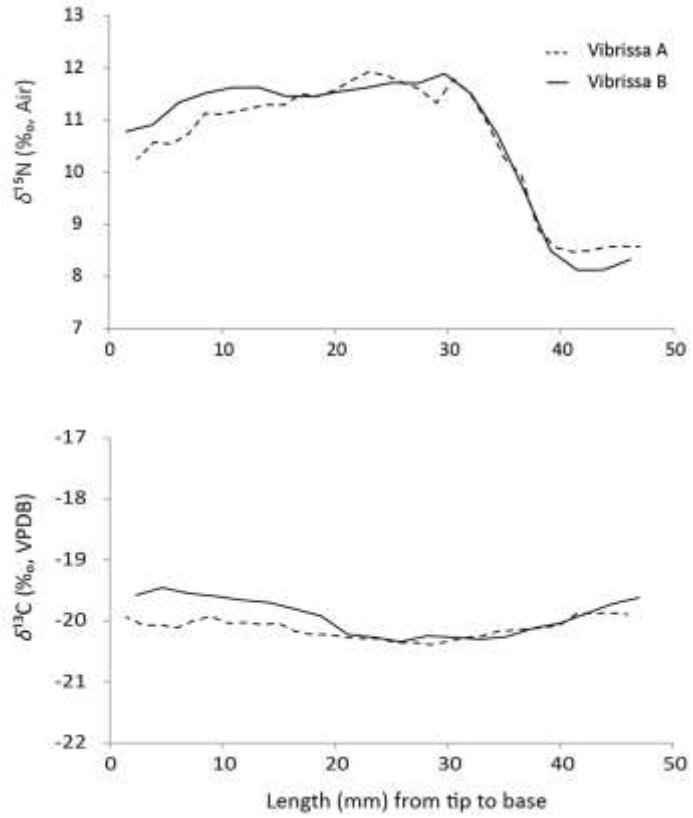

Figure 5: Synchronously grown vibrissal regrowths sampled from the same individual (Seal 3) were nearly identical, confirming that the SI data are similarly incorporated in different vibrissae.

Finally, the vibrissae collected from Seal 4 were used to assess the degree of synchronous vibrissal growth expected if the vibrissae were replaced synchronously. The eight vibrissae plucked from Seal 4 ranged from 73 to 165 mm in length and were sectioned into 352 total segments for SI analysis. The δ^{15}N ranged from 8.4 to 11.6 ‰ (9.7 ± 0.6 ‰). The δ^{13}C ranged from -19.4 to -21.7 ‰ (-20.3 ± 0.5 ‰). Significant differences in both δ^{15}N and δ^{13}C were detected among vibrissae (δ^{15}N: Kruskal-Wallis χ^2 = 64.4, df = 7, p < 0.001; δ^{13}C: Kruskal-Wallis χ^2 = 74.4, df = 7, p < 0.001). However, similarities in both δ^{15}N and δ^{13}C

between different vibrissae were obvious for Right C3, Right C4, and Left C5 (Figure 6), and the δ^{15}N pattern did not vary between most of the vibrissae, except for Right C1 and Right C5. The inter-vibrissal variation observable in δ^{13}C was also low; Right C5 had a unique δ^{13}C profile compared to the rest of the vibrissae.

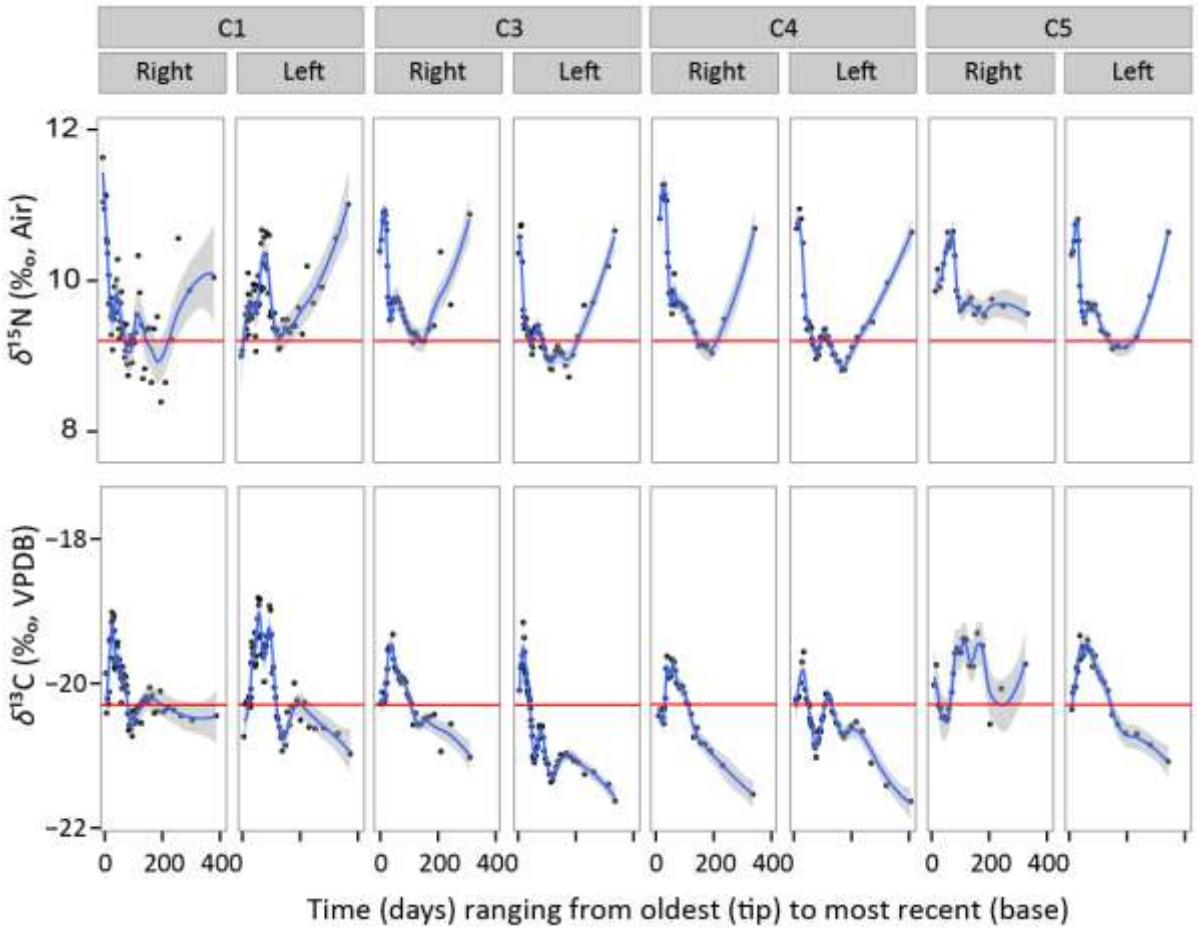

Figure 6: Time-series of δ^{15}N and δ^{13}C capture along the length of eight different vibrissae sampled from a dead adult female southern elephant seal (Seal 4). A Lowess smoothing algorithm was applied (grey). The arbitrary red line was added to ease comparison. The SI pattern of complementary vibrissae was similar.

Significant isotopic differences were detected between the proximal 10 mm, the adjacent 10 mm, and the most distal *ca.* 10 mm of the vibrissae (δ^{15}N: Kruskal-Wallis $\chi^2 = 52.3$, $df = 2$, $p < 0.001$; δ^{13}C: Kruskal-Wallis $\chi^2 = 36.0$, $df = 2$, $p < 0.001$; C:N: Kruskal-Wallis $\chi^2 = 14.5$, $df = 2$, $p < 0.001$) (Supplementary figure 2S). The C:N at the base and tip of vibrissae did not differ significantly ($p = 0.86$).

The atomic C:N ratio of all the vibrissal segments analysed (n = 596) was 3.7 ± 0.1.

DISCUSSION

Southern elephant seals show a greater probability of shedding most of their vibrissae during the annual moult than of retaining them. This finding contradicts the long-standing notion that SES vibrissae are shed asynchronously (Ling 1966). The timing of the SES synchronous vibrissal shedding was strongly related to the moult stage, being the highest near the completion of the moult (Figure 2). Yet, inter-individual variation in the vibrissal shedding during the moult precludes the inference of general assumptions regarding the growth history of fully grown vibrissae. This variability is likely due to the trade-offs between functionality and the need for replacement. Mammalian vibrissae function as individual, highly sensitive sensory organs vital to their foraging success, and an asynchronous loss-replacement strategy presumably allows for sustained functionality (Ling 1966; Greaves et al. 2004; Newland et al. 2011; Beltran et al. 2015). On the other hand, the moult may provide a period when vibrissae are redundant, given the land-based fasting typical of this species.

In this study, no individuals completely shed their vibrissae during the first moult (age one) (Supplementary figure 1S). Contrastingly, the majority of two-year old SES completely shed their vibrissae, consistent with the notion that phocid vibrissae can be retained for two years before being replaced (Ling 1966; Beltran et al. 2015). Previous studies suggested that full replacement of phocid vibrissae takes about one year (Hirons et al. 2001; Lewis et al. 2006; Beltran et al. 2015), although naturally-shed vibrissae could regrow in less than a full year (Hückstädt et al. 2011; Newland et al. 2011; Walters et al. 2014). New vibrissal regrowths were visible in 56.4 % of all the individuals that shed vibrissae during the 30.1 ± 9.7 day moulting period, suggesting that vibrissae can grow back rapidly (Supplementary figures,

plate 4S). One individual (Seal 5) that completely shed all its vibrissae was recaptured 138 days later with a full, although potentially still growing, vibrissal complement (Supplementary figures, plate 6S). Opportunistically sampled, fully grown vibrissae can, therefore, be up to two years old, but could have grown at any time.

Vibrissae that are shed and replaced simultaneously should incorporate a similar SI pattern along their lengths (e.g., Lewis et al. 2006). However, Hückstädt et al. (2011) and Newland et al. (2011) found contrasting results and subsequently describe the results of Lewis et al. (2006) as a sampling artefact. Nevertheless, the variable shedding patterns and similarities in isotopic signatures observed in some, but not all, vibrissae from Seal 4, help to explain the discrepancy between previous findings (Figure 6). Some of the vibrissae of Seal 4 appear to have grown synchronously after being shed. Nonetheless, we still have to assume the onset of the growth history of any randomly sampled vibrissa from an individual (especially considering the variability in the shedding probability between different aged SES – Supplementary figure 1S).

To control for unknown start and end dates of the biomolecule deposition (i.e. sampling vibrissae with unknown growth histories), we applied the von Bertalanffy growth function (von Bertalanffy 1938) to resampled vibrissae. With a Bayesian modelling approach, the vibrissal regrowth rate of the juvenile SES was shown to follow a nonlinear growth function with the growth rate decreasing as a function of length (Figure 3). The temporal resolution obtainable from the 2 mm vibrissal segments decreased exponentially from the tip (3.5 days) to the base of the vibrissae (> 40 days) as the growth rate decreased. The vibrissal regrowths were predicted to enter an inactive phase once the asymptotic length is reached, and had a similar lifespan to the vibrissae of *M. angustirostris* (*ca.* 369 days; Beltran et al. 2015).

Nevertheless, the vibrissal regrowths were still actively growing when sampled spanning the entire 363 ± 60.2 days of their first year spent at sea.

The vibrissal growth rate of pinnipeds range from 0.08 to 0.87 mm .day^{-1} (Hirons et al. 2001; Greaves et al. 2004; Zhao & Schell 2004; Hall-Aspland et al. 2005; Hindell et al. 2012).The SES vibrissal regrowth rates were within the predicted range of previous studies (Table 1). However, the regrowth rate of the juvenile SES vibrissae (K = 0.00744 day^{-1}, A = 77.1 mm) was higher than measured in other phocids, such as in captive juvenile grey seals *Halichoerus grypus* (K = 0.0024 day^{-1}, range = 0.0019 – 0.0030, A = 58.0 mm) (Greaves et al. 2004), the captive adult *M. angustirostris* (K = 0.00132 day^{-1}, range = 0.0045 – 0.00323, A = 81.7 mm) (Beltran et al. 2015), and adult leopard seals *Hydrurga leptonyx* (K = 0. 0032 day^{-1}, A = 72.0 mm) (Hall-Aspland et al. 2005). Still, the growth rate estimated from the simple linear regression was identical to the only other study of the vibrissal growth rate of juvenile SES (0.19 mm. d^{-1}, range 0.10 – 0.25 mm. d^{-1}) (Walters 2014), and similar to that of harbour seals *Phoca vitulina* (up to 0.78 mm d^{-1}) (Zhao & Schell 2004). However, the growth rate predicted by the von Bertalanffy growth function was higher than estimated by the simple linear model due to the non-linearity in growth (present study). Given the non-linear vibrissal growth rate, studies that relied on the presence of cyclic markers (e.g., annual fasting events or glycine markers) to measure the vibrissal growth rate of phocids might be unreliable, as they assumed that the vibrissal growth is linear and continuous (e.g., Hirons et al. 2001; Zhao & Schell 2004; Walters 2014); similarly noted in Greaves et al. (2004) and Hall-Aspland et al. (2005).

In the present study, inter-individual variation in the vibrissal regrowth rate was also evident (Figure 3). This may be constrained by the timing of the regrowth length measurements and sampling of vibrissae with different asymptotic lengths. Three or more measurements per individual are required to fit a non-linear vibrissal growth rate model. Furthermore, vibrissae

situated at different positions in the vibrissae bed-map have different *A's* and *K's*, which should be accounted for (e.g., Beltran et al. 2015). We sampled one of three mystacial vibrissae (Figure 1) due to the logistical challenge of sampling the same vibrissa from exactly the same position from different individuals in a wild population. This potentially contributed to the observed inter-individual variation in the vibrissal growth rates. Nevertheless, the resolution of dietary information obtainable with regrowths is higher than that obtainable from e.g., blood, hair, or any other tissue type collected from SES while foraging at sea for extended periods at a time.

Sampling considerations

Several unknowns regarding vibrissal growth remain. For instance, the increased somatic body growth of the pups could accelerate vibrissal regrowth rate, as observed in vibrissal regrowths collected from recently weaned bearded seal pups *Erignathus barbatus* (0.87 ± 0.24 mm. day^{-1}) (Hindell et al. 2012). Yet, the presence of the characteristic 3.4 ‰ δ^{15}N depletion from dependent nursing to independent foraging that was observable in the vibrissae of a 1.7 year old SES sampled at Marion Island, confirming that: a) the vibrissa growth ceases once the asymptotic length is reached, whereafter the growth enters a telogen phase; and b) their vibrissae are retained once the maximum length is reached before being replaced (Figure 3). This finding, and the unpredictable vibrissal growth histories of SES, suggests that the assumptions of previous studies might be invalid (e.g., Hückstädt et al. 2011; Newland et al. 2011). Newland et al. (2011), for example, utilised randomly selected 2 mm vibrissa segments of 1 – 3 year old SES to study the diet of juvenile SES at Macquarie Island (1999 – 2000). Yet, herein we demonstrate that the enriched δ^{15}N maternal signature, and subsequent δ^{15}N depletion at the onset of independent foraging (Walters et al. 2014), represents the majority of the vibrissae sampled from SES up to 1.7 years old (and perhaps

older), questioning their findings. The resampling of vibrissal regrowths not only accounts for growth history of the vibrissae, but also increases the portion of the vibrissa that represents independent foraging (Figure 4). Walters et al. (2014) sampled vibrissae of *ca.* 0.8 yo SES at Macquarie Island (54.6167° S, 158.8500° E), and merely 9.1 % of the total length of the vibrissae sampled from $n = 7$ out of 12 SES represented independent foraging. The portion representing independent foraging in the other individuals was still beneath the skin (Walters et al. 2014), similarly observed in the vibrissa of the previously unsampled Seal 1 (Figure 4).

In the present study, the longer, posterior vibrissae were generally retained, suggesting that the shorter vibrissae are more readily replaced (also see Ling 1966; Walters et al. 2014). Sampling the shorter, anterior (front) vibrissae, as suggested by Walters et al. (2014) and Beltran et al. (2015), increases the likelihood of it still being actively growing. Nonetheless, no accurate temporal interpretation of randomly sampled vibrissae is plausible if the growth histories are unknown. The sampling of vibrissae from juvenile SES should preferably occur as close as possible to departure on their post-weaning foraging trip, and regrowths can be resampled at the onset of their first obligatory moult.

The *ca.* 12 mm portion of the vibrissae left embedded when sampling the initial vibrissa captured the slowest part of the growth. The 12 mm portion could potentially represent *ca.* 130 days' growth (estimated from the von Bertalanffy growth function), which should be accounted for. The maximum growth rate of the vibrissae occurred directly after being cut, but will be represented 12 mm from the tip of the new regrowth due to the embedded 12 mm portion which still grew according to the initial vibrissa's growth curve (see Hall-Aspland et al. (2005).

Plucking vibrissal regrowths instead of cutting would add additional dietary information captured in the embedded 12 mm portion. Nevertheless, the cortical cells at the base of the vibrissae keratinize just above the bulb region of the follicle (within the internal root sheath) (Ling 1966), suggesting that the basal segment is still biologically active (growing) and does not represent pure keratin. As a result, the basal segments are mostly excluded from analyses (Hall-Aspland et al. 2005; Hückstädt et al. 2011; Beltran et al. 2015), suggesting that vibrissae plucking during sampling might be unnecessary. Although we found significant differences in the SI ratios between the base and the adjacent 10 mm of the vibrissae, similar differences between the base and the tip (Supplementary figure 2S) suggests that the variation might be caused by other biologically relevant factors, such as transition from active foraging and fasting during long distance migrations (e.g., Hückstädt et al. 2011), and requires further enquiry.

Lastly, when comparing the SI signature captured along the length of different vibrissae, it is assumed that the SI signature is incorporated similarly. The high reproducibility of the SI signature captured along the length of two synchronously grown vibrissal regrowths (Figure 5), and the vibrissae of Seal 4 (Figure 6), suggest that SI deposition is similar in different vibrissae with different growth rates (i.e. equal isotopic routing).

Conclusion

The use of vibrissal regrowths represents a feasible matrix for obtaining temporally integrated biogeochemical information. In general, the retention and shedding cycle of the vibrissae appears to be species- and individual-specific (Ling 1966; Greaves et al. 2004; Beltran et al. 2015). Although synchronous vibrissal shedding can occur in some individuals as demonstrated, no generalisation should be made regarding the period of biomolecule deposition in any vibrissae with an unknown growth history. In combination with the

unpredictable, asynchronous loss-replacement pattern (Ling 1966; Beltran et al. 2015), this hinders any verification of commencement of growth. Therefore, the growth history of vibrissae should be reset before temporal dietary interpretations are attempted. This study advances our capacity to interpret the interaction between predators and their environment on a biologically significant temporal scale.

ACKNOWLEDGEMENTS

Field personnel followed the guidelines for handling and treatment of marine mammals in field research supported by the Society for Marine Mammalogy (Gales et al. 2009). The tagging and handling of seals at Marion Island are carried out under the provisions of the South African Sea Birds and Seals Protection Act, 1973 (Act 46, 1973), the Marine Living Resources Act, 1998 (Act 18 of 1998) and the Prince Edward Islands Management Plan. The project has ethics clearance from the Animal Use and Care Committee (AUCC) of the Faculty of Veterinary Science, University of Pretoria, under AUCC 040827-022, AUCC 040827-023, AUCC 040827-024 and EC030602-016 and carried out under permit from the Director-General: Department of Environmental Affairs, South Africa.

Funding was provided by the South African Department of Science and Technology, through the National Research Foundation (NRF), within the South African National Antarctic Programme (SANAP). The Department of Environmental Affairs (DEA) provided logistical support at Marion Island. The opinions and conclusions drawn and discussed are attributed to the authors and not necessarily to the NRF. We thank the various dedicated collaborators, as well as field and laboratory assistants, in particular, Wiam Haddad, Mia Wege, Hennie Louw, Christiaan Brink, Frikkie van der Vyver, Dr Grant Hall, Nicolas Prinsloo, André van Tonder, Tanita Cronje, Inger Fabris-Rotelli, and Christine Kraamwinkel.

REFERENCES

Armstrong DP, Brooks RJ (2013) Application of hierarchical biphasic growth models to long-term data for snapping turtles. Ecol Model 250:119-125.

Banks J, Lea M-A, Wall S, McMahon CR, Hindell MA (2014) Combining bio-logging and fatty acid signature analysis indicates spatio-temporal variation in the diet of the southern elephant seal, *Mirounga leonina*. J Exp Mar Biol Ecol 450:79-90.

Beltran RS, Sadou MC, Condit R, Peterson SH, Reichmuth C, Costa DP (2015) Fine-scale whisker growth measurements can reveal temporal foraging patterns from stable isotope signatures. Mar Ecol Prog Ser 523:243-253.

Bester MN, de Bruyn PJN, Oosthuizen WC, Tosh CA, McIntyre T, Reisinger RR, Wege M (2011) The Marine Mammal Programme at the Prince Edward Islands: 38 years of research. Afr J Marine Sci 33:511-521.

Bester MN, Wilkinson IS (1994) Population ecology of southern elephant seals *Mirounga leonina* at Marion Island. In: Le Boeuf BJ, Laws RM (eds), *Elephant seals, population ecology, behavior, and physiology*. Berkeley and Los Angeles: University of California Press. pp 85-97.

Boecklen WJ, Yarnes CT, Cook BA, James AC (2011) On the use of stable isotopes in trophic ecology. Annu Rev Ecol Evol Syst 42:411-440.

Cherel Y, Ducatez S, Fontaine C, Richard P, Guinet C (2008) Stable isotopes reveal the trophic position and mesopelagic fish diet of female southern elephant seals breeding on the Kerguelen Islands. Mar Ecol Prog Ser 370:239-247.

Cherel Y, Kernaléguen L, Richard P, Guinet C (2009) Whisker isotopic signature depicts migration patterns and multi-year intra- and inter-individual foraging strategies in fur seals. Biol Lett 5:830-832.

Coplen TB (1994) Reporting of stable hydrogen, carbon, and oxygen isotopic abundances. Pure Appl Chem 66:273-276.

de Bruyn PJN, Tosh CA, Oosthuizen WC, Phalanndwa MV, Bester MN (2008) Temporary marking of unweaned southern elephant seal (*Mirounga leonina* L.) pups. S Afr J Wildl Res 38:133-137.

Gales NJ, Bowen WD, Johnston DW, Kovacs KM, Littnan CL, Perrin WF, Thompson PM (2009). Guidelines for the treatment of marine mammals in field research. Mar Mam Sci 25:725-736.

Greaves DK, Hammill MO, Eddington JD, Pettipas D, Schreer JF (2004) Growth rate and shedding of vibrissae in the Gray seal, *Halichoerus grypus*: A cautionary note for stable isotope diet analysis. Mar Mam Sci 20:296-304.

Grecian WJ, McGill RAR, Phillips RA, Ryan PG, Furness RW (2015) Quantifying variation in δ^{13}C and δ^{15}N isotopes within and between feathers and individuals: Is one sample enough? Mar Biol 162:733-741.

Hall-Aspland SA, Rogers TL, Canfield RB (2005) Stable carbon and nitrogen isotope analysis reveals seasonal variation in the diet of leopard seals. Mar Ecol Prog Ser 305:249-259.

Hindell MA, Lyderson C, Hop H, Kovacs KM (2012) Pre-partum diet of adult female bearded seals in years of contrasting ice conditions. PLoS ONE 7:e38307. doi: 10.1371/journal.pone.0038307.

Hirons AC, Schell DM, Aubin DJ (2001) Growth rates of vibrissae of harbor seals (*Phoca vitulina*) and Steller sea lions (*Eumetopias jubatus*). Can J Zool 79:1053-1061.

Hobson KA, Sinclair EH, York AE, Thomason JR, Merrick RE (2004). Retrospective isotopic analyses of Steller sea lion tooth annuli and seabird feathers: A cross-taxa approach to investigating regime and dietary shifts in the Gulf of Alaska. Mar Mam Sci 20:621-638.

Hückstädt LA, Burns JM, Koch PL, McDonald BI, Crocker DE, Costa DP (2012) Diet of a specialist in a changing environment: the crabeater seal along the western Antarctic Peninsula. Mar Ecol Prog Ser 455:287-301.

Hückstädt LA, Koch PL, McDonald BI, Goebel ME, Crocker DE, Costa DP (2011) Stable isotope analyses reveal individual variability in the trophic ecology of a top marine predator, the southern elephant seal. Oecologia 169:395-406.

Hussey NE, Kessel ST, Aarestrup K, Cooke SJ, et al. (2015) Aquatic animal telemetry: A panoramic window into the underwater world. Science 348: 1255642. doi:10.1126/science.1255642.

Jaeger A, Jaquemet S, Phillips RA, Wanless RM, Richard P, Cherel Y (2013) Stable isotopes document inter- and intra-specific variation in feeding ecology of nine large southern Procellariiformes. Mar Ecol Prog Ser 490:255-266.

Kernaléguen L, Cazelles B, Arnould JPY, Richard P, Guinet C, et al. (2012) Long-term species, sexual and individual variations in foraging strategies of fur seals revealed by stable isotopes in whiskers. PLoS ONE 7(3): e32916. doi:10.1371/journal.pone.0032916.

Kirkman SP, Bester MN, Pistorius PA, Hofmeyr GJG, Jonker FC, Owen R, Strydom N (2003) Variation in the timing of moult in southern elephant seals at Marion Island. S Afr J Wildl Res 33:79-84.

Lewis R, O'Connell TC, Lewis M, Campagna C, Hoelzel AR (2006) Sex-specific foraging strategies and resource partitioning in the southern elephant seal (*Mirounga leonina*). Proc Biol Sci 273:2901-2907.

Ling JK (1966) The skin and hair of the southern elephant seal, *Mirounga leonina* (Linn.) I. The facial vibrissae. Aust J Zool 14:355-866.

Lowther AD, Harcourt RG, Goldsworthy SD (2013) Regional variation in trophic ecology of adult female Australian sea lions inferred from stable isotopes in whiskers. Wildlife Res 40:303-311.

McHuron EA, Walcott SM, Zeligs J, Skrovan S, Costa DP, Reichmuth C (2016) Whisker growth dynamics in two North Pacific pinnipeds: implications for determining foraging ecology from stable isotope analysis. MEPS 554: 213-224.

McMahon KW, Hamady LL, Thorrold SR (2013) A review of ecogeochemistry approaches to estimating movements of marine animals. Limnol Oceanogr 58:697-714.

Newland C, Field IC, Cherel Y, Guinet C, Bradshaw CJA, McMahon CR, Hindell MA (2011) Diet of underyearling southern elephant seals reappraised by stable isotopes in whiskers. Mar Ecol Prog Ser 424:247-258.

Pistorius PA, de Bruyn PJN, Bester MN (2011) Population dynamics of southern elephant seals: a synthesis of three decades of demographic research at Marion Island. African J Mar Sci 33:523-534.

Postma M, Bester MN, de Bruyn PJN (2013) Age-related reproductive variation in a wild marine mammal population. Polar Biol 36:719-729.

R Development Core Team (2013) R: A language and environment for statistical computing. R Foundation for Statistical Computing, Vienna, Austria. ISBN 3-900051-07-0, URL http://www.R-project.org.

Rea LD, Christ AM, Hayden AB, Stegall VK, Farley SD, et al. (2015) Age-specific vibrissae growth rates: A tool for determining the timing of ecologically important events in Steller sea lions. Mar Mam Sci 31:1213-33.

Robertson A, McDonald RA, Delahay RJ, Kelly SD, Bearhop S (2012) Whisker growth in wild Eurasian badgers *Meles meles*: implications for stable isotope and bait marking studies. Eur J Wildl Res 59:341-350.

Rohwer S, Ricklefs RE, Rohwer VG, Copple MM (2009) Allometry of the duration of flight feather molt in birds. PLoS Biol. 7(6):e1000132.

Sadou MC, Beltran RS, Reichmuth C (2014) A calibration procedure for measuring pinniped vibrissae using photogrammetry. Aquat Mam 40:213-218.

Tieszen LL, Boutton TW, Tesdahl KG, Slade NA (1983) Fractionation and turnover of stable carbon isotopes in animal tissues: implications for $\delta^{13}C$ analysis of diet. Oecologia 57:32-37.

von Bertalanffy L (1938) A quantitative theory of organic growth. Human Biol 10:181-213.

Walters A (2014) Quantifying the trophic linkages of Antarctic marine predators. PhD thesis. University of Tasmania.

Walters A, Lea M-A, van den Hoff J, Field IC, Virtue P, Sokolov S, Pinkerton MH, Hindell MA (2014) Spatially explicit estimates of prey consumption reveal a new krill predator in the Southern Ocean. PLoS ONE 9: e86452. dio: 10.1371/journal.pone.0086452.

Wilkinson IS, Bester MN (1990) Duration of post-weaning fast and local dispersion in the southern elephant seal, *Mirounga leonina*, at Marion Island. J Zool 222:591-600.

Young JW, Hunt BPV, Cook TR, Llopiz JK, Hazen EL, Pethybridge HR, et al. (2015) The trophodynamics of marine top predators: Current knowledge, recent advances and challenges. Deep Sea Res Part II: Top Stud Oceanogr 113:170-187.

Zhao L, Schell DM (2004) Stable isotope ratios in harbor seal *Phoca vitulina* vibrissae: effects of growth patterns on ecological records. Mar Ecol Prog Ser 281:267-273.

Supplementary material

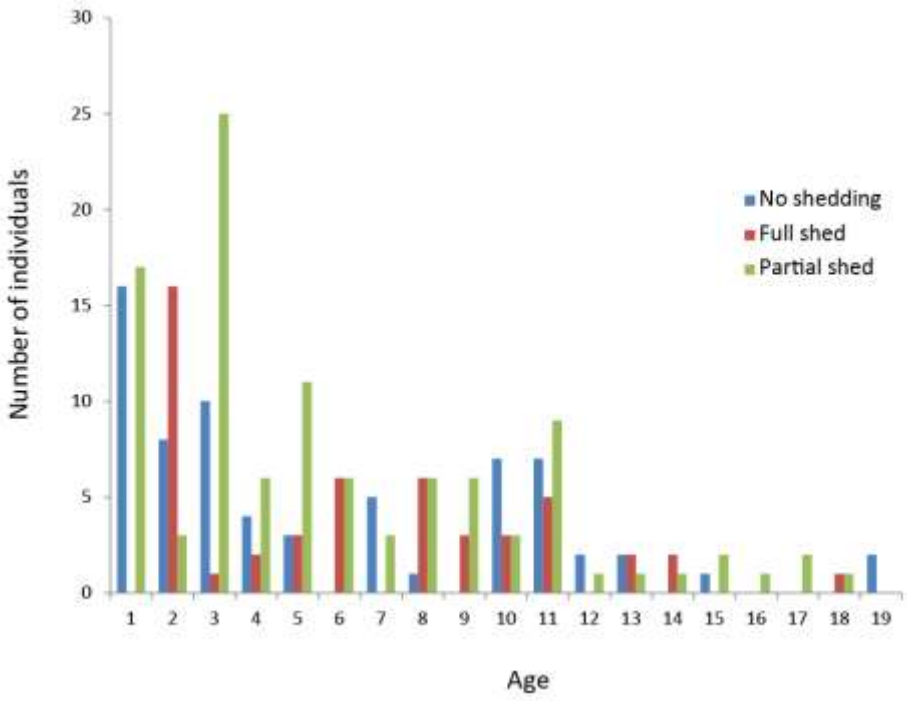

Figure 1S: Number of individual southern elephant seals included per age-class that shed, partially shed, or displayed no signs of vibrissal shedding.

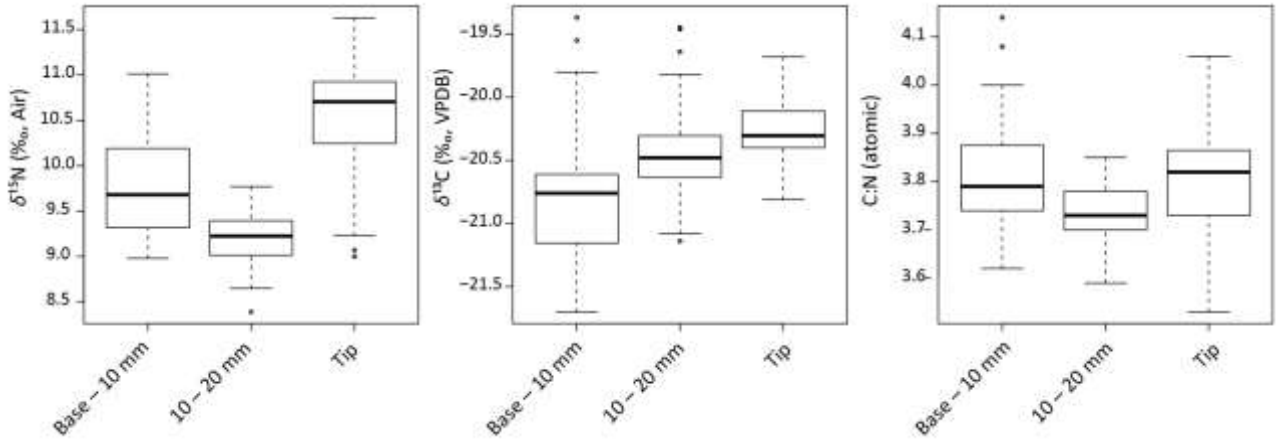

Figure 2S: The isotopic signature captured in the base of the plucked vibrissae was significantly different from the adjacent 10 mm ($p < 0.001$), likely due to the presence of molecules other than keratin (Seal 4).

Plate 1S: The atypical, synchronous vibrissal shedding of southern elephant seals observed during post-moult satellite-tag deployments on Marion Island. The vibrissae were either completely (left), partially (middle) shed, or not shed (right).

Plate 2S: Example of a southern elephant seal with a full complement of mystacial vibrissae, photographed during the winter resting haulout.

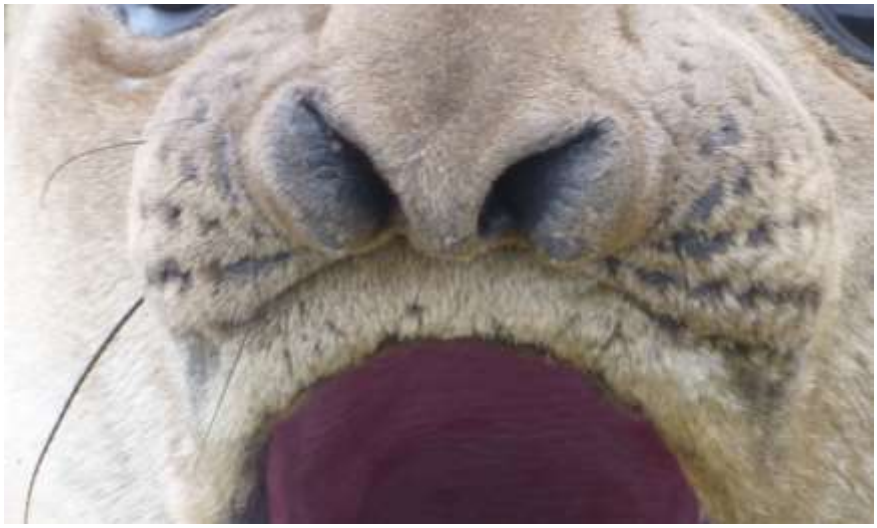

Plate 3S: Example of a southern elephant seal that completely shed its vibrissae during the annual pelage moult.

Plate 4S: Example of a southern elephant seal that completely shed its vibrissae during the annual pelage moult, with new vibrissal regrowths visible. Only two prominent vibrissae were retained and fine, new vibrissal regrowths are observable shortly after shedding suggesting that vibrissae replacement occurs rapidly.

Plate 5S: Example of the vibrissal regrowths collected from a juvenile southern elephant seal. Regrowths are easy to identify visually due to their blunt, large diameter distal ends (indicated by the red arrow).

Plate 6S: Vibrissal shedding and replacement observed in a juvenile southern elephant seal (Seal 5). After arriving for the annual moulting period (left) with a full vibrissal complement, the vibrissae were completely shed during the post-moult period (middle). New vibrissal regrowths were already observable during the post-moult period (middle). However, this individual was recaptured four months later (138 days) with a full complement of vibrissae (right), albeit that the vibrissae were still growing.